

## Photoproduction of Neutral Pions from Hydrogen in the Energy Range 700–1100 Mev\*

H. H. BINGHAM AND A. B. CLEGG†  
*California Institute of Technology, Pasadena, California*

(Received August 19, 1958)

Gamma-rays from the decay of neutral pions photoproduced from hydrogen by the bremsstrahlung beam of the Caltech synchrotron have been studied with a thallium chloride crystal total absorption spectrometer. The energy spectrum of the decay gamma-rays produced by a range of incident photon energy is obtained by the photon difference method and this spectrum enables a separation of the gamma-rays into two groups: (i) those from the decay of neutral pions produced singly from hydrogen and (ii) those from the decay of neutral pions from multiple-production reactions. The cross sections for the single-production reaction are in agreement with the recoil proton experiments at Caltech and Cornell. For the multiple-production reactions we measure the cross section for producing neutral pions within a range of kinetic energies:

Incident photon energy	Center-of-mass angle	$\pi^0$ kinetic energy range (c.m.)	$d\sigma/d\Omega$ (c.m.), in $\text{cm}^2 \text{sterad}^{-1}$
990 Mev	91°	175 Mev to 360 Mev	$(5.9 \pm 1.6) \times 10^{-30}$
990 Mev	118°	80 Mev to 360 Mev	$(8.1 \pm 1.9) \times 10^{-30}$
810 Mev	114°	75 Mev to 290 Mev	$(3.7 \pm 1.0) \times 10^{-30}$

It is shown that all available multiple-production data can be explained in terms of two compound states, one at about 750 Mev and the other at some higher energy. This is in agreement with an analysis of the single-photoproduction data, which is given in an appendix. These two states are, respectively, ( $T = \frac{1}{2}, J = \frac{1}{2}+$ ) and ( $T = \frac{3}{2}, J = \frac{1}{2}+$ ).

### I. INTRODUCTION

RECENTLY several experiments have been done to study the single production of neutral pions:

$$\gamma + p \rightarrow p + \pi^0,$$

in the energy range 500–1100 Mev, by observing the recoil proton<sup>1-3</sup> or a coincidence between the recoil proton and one of the gamma-rays from the decay of the neutral pion.<sup>4</sup> In the experiment described here we have observed the gamma-rays from the decay of neutral pions produced both in this reaction and in multiple-production reactions, typically:

$$\gamma + p \rightarrow n + \pi^+ + \pi^0,$$

$$\gamma + p \rightarrow p + \pi^0 + \pi^0, \text{ etc.}$$

The energy spectrum of the outgoing gamma-rays produced by a range of approximately 200 Mev of incident photon energy is observed by the photon difference method. From this spectrum we deduce the corresponding neutral pion energy spectrum which enables the separation of the neutral pions into two groups: those produced in the single-production reaction and those produced in multiple-production reactions. This is possible, even with a low-resolution gamma-ray spectrometer as is used in this experiment, because of the considerable simplicity of the gamma-ray spectrum from the decay of the monoenergetic neutral pions produced in the single-production reaction.

It has been noted by Sternheimer<sup>5</sup> that if one observes a gamma-ray of energy greater than 200 Mev from the

decay of a neutral pion, the pion must have been travelling in a direction less than 20° from the direction at which the gamma-ray is observed. So, as gamma-rays with energies greater than 200 Mev are studied in this experiment, the gamma-ray spectrometer acts effectively as a neutral-pion spectrometer with a coarse angular resolution.

In Sec. VII we give an analysis of the meager multiple pion photoproduction data in terms of two compound states. This analysis is guided by a similar naive analysis of single pion photoproduction by one of us (A.B.C.) which is described in an appendix.

### II. APPARATUS AND PROCEDURE

#### Beam and Target

The arrangement of bremsstrahlung beam and liquid hydrogen target is the same as that used by Donoho and Walker.<sup>6</sup> The bremsstrahlung beam is collimated to a rectangular cross section of  $5.1 \times 6.3 \text{ cm}^2$  and the liquid hydrogen is contained in a cylindrical Mylar cup three inches in diameter, which is surrounded by a vacuum chamber; the outer wall of the vacuum chamber and the radiation shields are far enough from the liquid hydrogen to contribute very little to the background. The gamma-ray spectrometer can be rotated about a pivot placed under the hydrogen target so as to observe the yield of gamma-rays at different angles to the bremsstrahlung beam. Under normal operating conditions the beam intensity is about 1 to  $2 \times 10^{11}$  Mev per pulse with one pulse per sec; each beam pulse is spilled uniformly over a time of about twenty msec. The beam monitor was calibrated<sup>7</sup> with a quantummeter of the type described by Wilson.<sup>8</sup> The bremsstrahlung spectrum has been measured with a pair

\* This work was supported in part by the U. S. Atomic Energy Commission.

† Now at Clarendon Laboratory, Oxford, England.

<sup>1</sup> J. I. Vette, Phys. Rev. **111**, 622 (1958).

<sup>2</sup> R. M. Worlock, Ph.D. thesis, California Institute of Technology, 1958 (unpublished).

<sup>3</sup> P. C. Stein and K. C. Rogers, Phys. Rev. **110**, 1209 (1958).

<sup>4</sup> DeWire, Jackson, and Littauer, Phys. Rev. **110**, 1208 (1958).

<sup>5</sup> R. M. Sternheimer, Phys. Rev. **99**, 277 (1955).

<sup>6</sup> P. L. Donoho and R. L. Walker, Phys. Rev. **112**, 981 (1958).

<sup>7</sup> R. Gomez (unpublished report).

<sup>8</sup> R. R. Wilson, Nuclear Instr. **1**, 101 (1957).

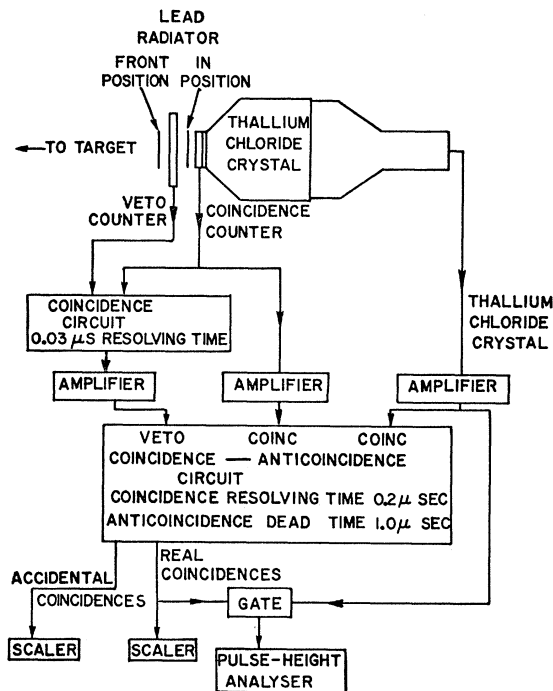


FIG. 1. Block diagram of gamma-ray telescope and electronic equipment.

spectrometer,<sup>9</sup> and was found to be a thin-target spectrum, within the errors, except that no rounding-off was observed at the high-energy end, within the energy resolution:  $\Delta k/k = 0.02$ .

### Gamma-Ray Spectrometer

The gamma-ray spectrometer consists primarily of a cylindrical single crystal of thallium chloride<sup>10</sup> with a length of 13.4 radiation lengths. This crystal is large enough to absorb a large part of the energy of an electron-photon shower, the electrons of the shower producing Čerenkov light which is observed by a photomultiplier. The testing of this counter is described in Sec. III. So as only to count gamma-rays incident within one inch of the axis of the crystal, this counter was used in a gamma-ray telescope; a diagram of this telescope together with a block diagram of the electronic equipment is shown in Fig. 1. In front there is a four-inch diameter veto scintillation counter to reject charged particles, particularly fast pions which produce Čerenkov light in the thallium chloride crystal (a pion of energy 200 Mev or greater passes through the crystal and produces a pulse as big as that produced by a 200-Mev electron-photon shower). The veto counter is followed by a radiator, of lead of thickness 0.371 cm in normal operation, a two-inch diameter coincidence

scintillation counter and finally the crystal. A bias was set on the coincidence counter to accept pulses corresponding to at least two electrons passing through it. When there was a coincidence between the coincidence counter and the crystal with no count in the veto counter the corresponding pulse from the crystal was observed with a twenty-channel pulse-height analyzer. Runs were made with the lead radiator in front of the coincidence counter (the IN position) and in front of the veto counter (the FRONT position). The difference between these results corresponds to gamma-rays converting in the lead radiator; a count will occasionally be lost when one of the electrons of the initial pair fails to get through the radiator and into the scintillation counter. It was checked that the IN-minus-FRONT counting rate varied correctly on changing the thickness of the lead radiator and on changing to radiators of aluminum, copper and tin. The counting rate from the FRONT position, primarily due to conversion of gamma-rays in the scintillation counters, was small: one-tenth or less of the counting-rate from the IN position. This procedure of taking IN-minus-FRONT differences rather than the more usual IN-minus-OUT differences was chosen so as to leave the flux of particles incident on the two rear counters the same, thus providing a more accurate subtraction of accidentals. In the one case a comparison was made, the IN-minus-FRONT spectrum was found to be the same as the IN-minus-OUT spectrum.

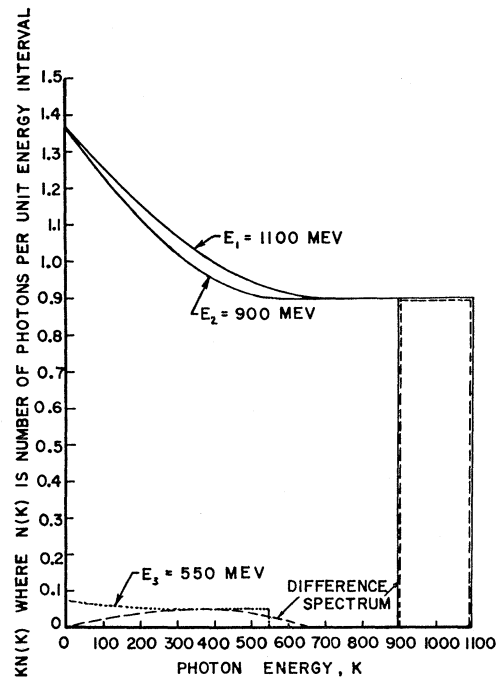


FIG. 2. Illustration of photon difference method.

<sup>9</sup> Donoho, Emery, and Walker (private communication).

<sup>10</sup> Supplied by Mr. Newell F. Blackburn, Engineer Research and Development Laboratories, Fort Belvoir, Virginia.

### Experimental Procedure

Data were taken at two synchrotron energies separated by about 200 Mev and the yield at the lower energy, after appropriate normalization, subtracted from the yield at the higher energy. As the pulse-height spectrum from the gamma-ray spectrometer is approximately exponential at any synchrotron energy, the accuracy of the subtraction is critically dependent on the stability of the gain of the system. This was checked by running on each day of operation first at one energy, then at the second, and finally back at the first. This would show whether there was an appreciable shift in gain during the day and otherwise cancelled out errors due to small unobserved shifts. Each point was run in this way on at least two different days and consistency was required between the different sets of data. When care was taken in this way, the stability of the standard high-voltage power-supplies and amplifiers in use in this laboratory was found adequate for this work. Every night a run was made with cosmic-ray muons passing through the thallium chloride crystal in a standard geometry; as described in Sec. III, to calibrate the gain of the counter. Runs were made with the hydrogen target full and empty; the empty-target counting rate was only a few percent of the full-target counting rate and was subtracted out.

### Photon Difference Method

The details of the subtraction are illustrated in Fig. 2. The bremsstrahlung spectra corresponding to synchrotron energies  $E_1$  and  $E_2$  are normalized so that they give the same number of photons of energy  $E_2$ . The difference between the yields thus normalized will be the yield due to photons of energies between  $E_1$  and  $E_2$  together with the yield due to a weak intensity of lower energy photons. We want to correct for the latter, leaving the yield due to photons of energies between  $E_1$  and  $E_2$ . A close approximation to this correction was directly measured by operating the synchrotron at an energy  $E_3$ . The necessary small correction to this

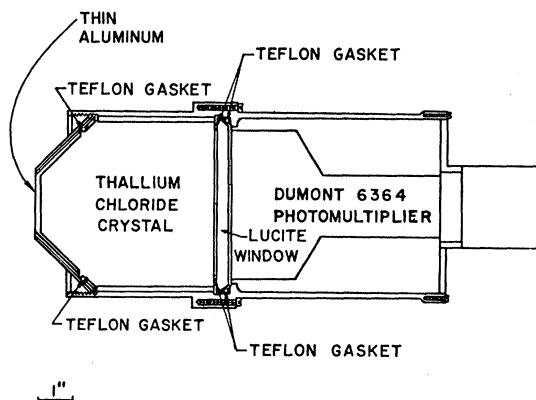


FIG. 3. Thallium chloride crystal and mounting.

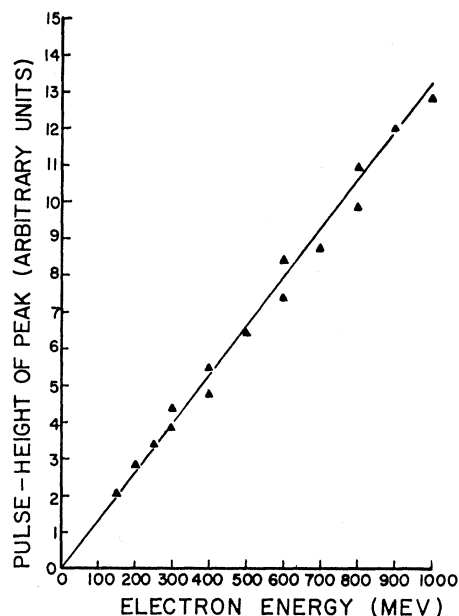


FIG. 4. Energy response of thallium chloride crystal counter for monoenergetic electrons.

measurement was calculated using the known neutral pion cross sections.<sup>1</sup>

### III. TESTS OF GAMMA-RAY SPECTROMETER

The thallium chloride crystal is 5.5 in. long and 5.75 in. in diam. and it has a radiation length of 1.04 cm. The crystal and its mounting case are shown in Fig. 3. The surface of the crystal is polished, except for the face towards the photomultiplier which is left rough; the surface is wrapped with aluminum foil in an attempt to preserve the predominantly forward momentum of the Čerenkov light.

The counter was tested using electrons produced in a lead target by the bremsstrahlung beam and analyzed in momentum by a magnet.<sup>11</sup> The electrons passed through a two-in. diam scintillation counter into the crystal so that the pulse from the crystal was observed on a pulse-height analyzer when there was a coincidence with the scintillation counter. Thus we were studying the effect of electrons incident within one inch of the axis. In this arrangement the momentum spread of the electrons was about 5%. For each electron energy we measured the pulse-height and width of the resulting peak in the pulse-height spectrum; the width quoted is the full width at half maximum, corrected for the momentum spread of the electrons.

The energy response is shown in Fig. 4: there is no large departure from linearity up to 1000 Mev, which is perhaps surprising, as one might expect a large proportion of the energy of the shower, perhaps 40% or more, to be escaping from the crystal at such energies.

<sup>11</sup> We are indebted to Dr. R. L. Walker for the use of this equipment.

There is, however, a possible compensating effect: we find that the light collection efficiency for fast charged particles travelling towards the photocathode is better by a factor of nearly two than that for particles crossing the crystal along a diameter, a result which might be expected due to the directional properties of Čerenkov light. So for higher energy showers one could expect a higher proportion of the electron track to be towards the photocathode, causing the light collection efficiency to increase with energy.

During these runs the pulse height produced by electrons of known energy was compared with the pulse height produced by cosmic-ray muons passing through the crystal in a standard geometry defined by requiring them to pass through two scintillation counters, so that a repeat of the cosmic-ray run could be used to establish the energy calibration as described in Sec. II.

The variation of width with electron energy is shown in Fig. 5 where the square of the width is plotted against the reciprocal of the electron energy. If the width is primarily due to statistical fluctuations in the photomultiplier, the points should lie on a straight line through the origin. It would seem that this is approximately so for electron energies less than 350 Mev. This implies a light collection efficiency of about 35%, which means that an average of about 43 electrons are produced at the photocathode for every 100 Mev in the shower. Kantz and Hofstadter<sup>12</sup> have described a model for the escape of the fringe of a shower as the escape of gamma-rays at the energy of the absorption minimum, the fluctuation in the number of gamma-rays

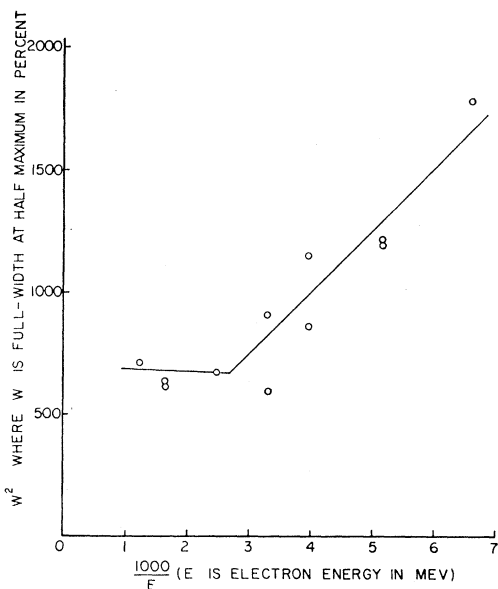


FIG. 5. Resolution of thallium chloride crystal counter for monoenergetic electrons.

<sup>12</sup> A. Kantz and R. Hofstadter, *Nucleonics* 12, No. 3, 36 (1954).

contributing to the width. If the energy escaping in this way is proportional to the total energy of the shower the width varies in the same way as above. However, estimates of the magnitude of this effect indicate a width one-half or less than we observe, implying that our resolution is primarily due to photomultiplier statistics. The larger widths at energies above 350 Mev are presumably due to escape of an appreciable proportion of the shower from the crystal.

When electrons are incident on the crystal at distances greater than one inch from the axis, the resolution is distinctly worse, so it was used in a gamma-ray telescope as described in Sec. II. The resolution for monoenergetic gamma-rays was calculated from the observed resolution for monoenergetic electrons.

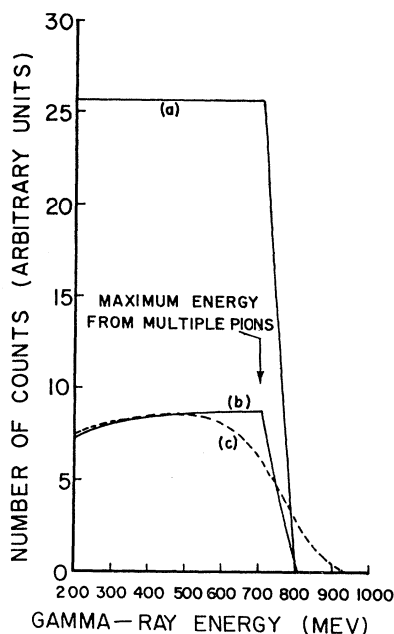


FIG. 6. Illustration of calculation of pulse-height spectrum due to gamma-rays from the decay of neutral pions photoproduced singly by a range of 200 Mev of incident photon energy. (a) Calculated gamma-ray energy spectrum. (b) After multiplying (a) by efficiency of gamma-ray telescope. (c) After smearing (b) with counter resolution: the calculated pulse-height spectrum.

#### IV. NEUTRAL PION DECAY KINEMATICS

Consider  $N$  monoenergetic neutral pions emitted isotropically from a source with energy  $E$  and velocity  $\beta$ , such as might be produced by monoenergetic photons interacting with protons in the center-of-momentum system of photon and proton. Then the number of pions emitted into the solid angle between  $\theta$  and  $\theta + d\theta$  is  $\frac{1}{2}N \sin\theta d\theta$ . On decaying, these neutral pions emit  $(1-\beta^2)d\Omega/[2\pi(1-\beta \cos\theta)^2]$  photons of energy

$$h = \mu(1-\beta^2)^{\frac{1}{2}}/[2(1-\beta \cos\theta)]$$

into solid angle  $d\Omega$  at  $\theta=0$ , where  $\mu$  is the rest mass of the pion. Then the energy spectrum of decay photons

observed at  $\theta=0$  due to the  $N$  original pions is

$$P(k)dk = \frac{1}{2}N \sin\theta \frac{1-\beta^2}{2\pi(1-\beta \cos\theta)^2} d\Omega \left(\frac{dk}{d\theta}\right)^{-1} dk$$

$$= N \frac{(1-\beta^2)^{\frac{1}{2}}}{2\pi\mu\beta} d\Omega dk.$$

Thus the energy spectrum is a rectangle extending from energy  $\delta$  to energy  $(E-\delta)$ , with  $\delta \approx \mu^2/4E$  for large  $E$ .  $\delta$  is only a few Mev when  $E$  is several hundred Mev, so it is only a small approximation to take  $\delta$  to be zero. Next we note that the observation of a gamma-ray of energy greater than 200 Mev implies the parent pion was at an angle less than  $20^\circ$  from the direction of observation, so we can disregard the assumption of isotropy of emission of the pion and we have a rectangular gamma-ray spectrum from 200 Mev to  $(E-\delta)$  from monoenergetic pions within  $20^\circ$  of the direction of observation. For a pion energy spectrum  $f(k)$ , in the approximation that  $\delta=0$ , we obviously get the formula derived by Sternheimer<sup>5</sup>:

$$f = -k(\partial P/\partial k).$$

TABLE I. Cross sections for single neutral-pion photoproduction.

Photon energy (Mev)	Laboratory angle	Center-of-mass angle	$d\sigma/d\Omega$ (c.m.) (cm <sup>2</sup> sterad <sup>-1</sup> )
980	45°	72°	$(1.63 \pm 0.21) \times 10^{-30}$
990	60°	91°	$(1.53 \pm 0.64) \times 10^{-30}$
990	86°	118°	$(2.89 \pm 0.47) \times 10^{-30}$
810	86°	114°	$(3.25 \pm 0.34) \times 10^{-30}$

Finally, one must transform from the center-of-momentum system of the target proton and incident photon to the laboratory system. An outgoing photon of energy  $k$  at an angle  $\psi$  to the incident photon beam transforms into a photon of energy  $k'$  at an angle  $\psi'$  in the laboratory:

$$k' = k(1 + \beta' \cos\psi)/(1 - \beta'^2)^{\frac{1}{2}},$$

$$\cos\psi' = (\beta' + \cos\psi)/(1 + \beta' \cos\psi),$$

where  $\beta'$  is the relative velocity of the two systems. Thus, all the photons at one angle  $\psi$  in the center-of-momentum system are transferred to one angle  $\psi'$  in the laboratory system and the energy spectrum is simply expanded or contracted uniformly.

## V. RESULTS

For a range of 200 Mev of incoming photon energy, the neutral pions from single production fall within a narrow range of energy, while the pions from multiple production all have energies lower than this range. Assuming the cross section for single production to be uniform across the range of incident photon energy, it is easy, from the discussion of the last section, to

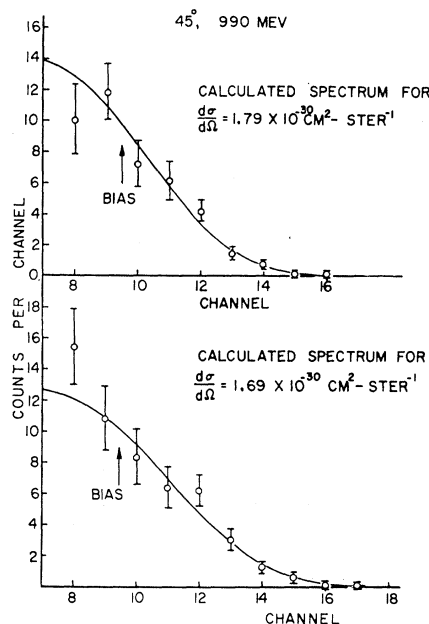


FIG. 7. Examples of fits of calculated spectrum to experimental spectra. Cross sections quoted are not corrected for empty target background.

calculate the gamma-ray energy spectrum corresponding to single production, with arbitrary normalization. This is then multiplied by the telescope efficiency, which is primarily the probability of pair production in the lead radiator with a correction of a few percent for the possibility of one of the two electrons not getting through into the coincidence counter. We used the calculations of Davies *et al.*<sup>13</sup> for the pair production cross section. This spectrum is then smeared with the counter resolution. The three steps of this calculation are illustrated in Fig. 6. This calculated pulse-height spectrum is normalized to fit the data (the energy calibration being taken from the cosmic-ray runs) above a bias chosen so that multiple production could not contribute. Examples of two such fits are shown in Fig. 7. From the normalization the cross section is calculated; results are shown in Table I. The errors are primarily a combination of counting statistics and of uncertainty in the energy calibration, this last being mainly due to uncertainty in determining the position of the peak in the pulse-height spectrum in the cosmic-ray runs.

The results are compared in Figs. 8 and 9 with the experiments observing recoil protons in this laboratory<sup>1,2</sup>; the data obtained at Cornell<sup>3,4</sup> are quite consistent with these results. The agreement between our data and these other experiments is comforting as completely different techniques are used. In our experiment the identification of single production is unambiguous, while in the recoil proton experiments there

<sup>13</sup> Davies, Bethe, and Maximon, Phys. Rev. 93, 788 (1954).

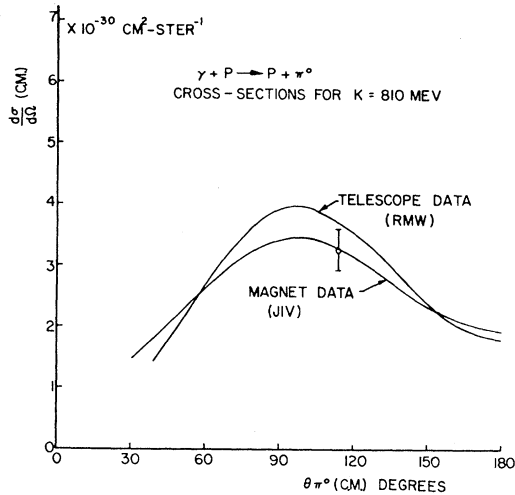


FIG. 8. Comparison of single-production result at 810 Mev for this experiment with those from recoil-proton experiments in this laboratory.<sup>1,2</sup> Curves shown are polynomials in  $\cos\theta$  fitted to recoil-proton data by least squares.

is a background of protons from multiple production which has to be subtracted. However, the recoil proton experiments have a real advantage in speed of gathering data.

After subtracting these calculated spectra from the experimental data, we find residual counts due to multiple production reactions. Taking these results we divide the counts in each channel by the efficiency for observing gamma-rays of that energy to obtain the actual gamma-ray spectrum and from this we calculate the corresponding pion energy spectrum using the formula obtained in Sec. IV. In practice an approximation was used.

$$f_i = -\frac{k_i + k_{i+j}}{4} \left( \frac{P_i - P_{i+j}}{k_i - k_{i+j}} \right),$$

where  $P_i$  is the number of gamma-rays in channel  $i$  and  $k_i$  is the gamma-ray energy corresponding to the

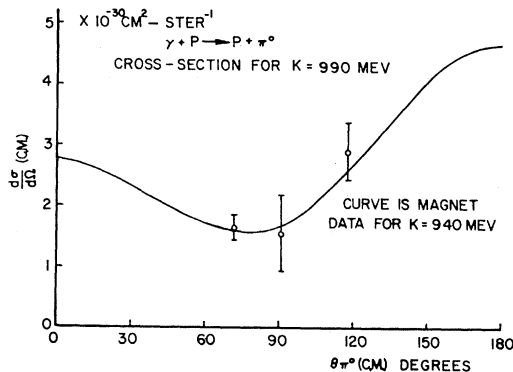


FIG. 9. Comparison of single-production results at 990 Mev in this experiment with those from the recoil-proton experiment at 940 Mev in this laboratory.<sup>1</sup> Curve shown is polynomial in  $\cos\theta$  fitted to recoil-proton data by least squares.

lower limit of that channel.  $f_{ij}$  corresponds to the yield of pions with total energies between  $k_i + \delta_i$  and  $k_{i+j} + \delta_{i+j}$  where  $\delta_i$  is that referred to in Sec. IV. Because of the poor statistics after all the subtractions, we have chosen  $j$  so as to split the data only into two groups of pion energies; the results are given in Table II. A summary is given in Table III of the cross section for producing pions, with kinetic energies between two limits, in multiple production reactions. The lower limit is set by the experiment while the upper is set by the kinematics. The cross section quoted is a sum over the cross sections for all possible multiple-production reactions, each cross section being weighted by the number of neutral pions produced in the reaction.

## VI. ALTERNATIVE POSSIBLE GAMMA-RAY SOURCES

We have assumed that the gamma-rays observed come from the decay of neutral pions. A possible alternative source is elastic scattering of gamma-rays from the proton. This would produce a gamma-ray line at approximately the peak energy we see. The number of counts observed at this energy puts an upper limit on the intensity of such a line and this implies that the elastic scattering cross section is less than one-fifth of the cross sections quoted for single production. From extrapolations of an experiment<sup>14</sup> and calculations<sup>15,16</sup> that have been done at lower energies, one expects the actual cross section to be distinctly smaller than this, so we have ignored elastic scattering as a possible contributor to our yield.

There is also the possibility that another neutral meson, hitherto unidentified, which decays into gamma-rays might be involved. One such is the spin-one meson suggested by Nambu.<sup>17</sup> If photoproduced singly from the proton, the total energy and momentum of this meson are both very weak functions of the mass assumed for it. We have calculated the gamma-ray energy spectrum from its decay and find that it can be fitted to our data. The cross section for photoproduction of this new meson determined by fitting this gamma-ray spectrum to our observations is about three times that deduced from the observation of recoil protons.<sup>1-3</sup> So this discrepancy implies that such a meson cannot be a major contributor to our data. The agreement between our experiment and the recoil proton experiments implies that the cross section for producing Nambu's meson must be less than one-fifth of that for producing neutral pions.

Because the total energy of a meson photoproduced singly is a weak function of its mass we can say very little about the possibility that other spin-zero mesons

<sup>14</sup> L. B. Auerbach *et al.*, *Proceedings of the CERN Symposium on High-Energy Accelerators and Pion Physics, Geneva, 1956* (European Organization of Nuclear Research, Geneva, 1956), Vol. 2, p. 291.

<sup>15</sup> R. H. Capps, *Phys. Rev.* **106**, 1031 (1957).

<sup>16</sup> Karzas, Watson, and Zachariasen, *Phys. Rev.* **110**, 253 (1958).

<sup>17</sup> Y. Nambu, *Phys. Rev.* **106**, 1366 (1958).

decaying into two gamma-rays, might be involved, except that the mass cannot be greater than about 250 Mev from the end-point energy observed in the gamma-ray spectra.

VII. DISCUSSION OF PION PAIR PRODUCTION

The energy spectra of negative pions photoproduced from hydrogen<sup>18</sup> suggests the importance of an isobar model, where a  $T=\frac{3}{2}$ ,  $J=\frac{3}{2}$  isobar is produced together with a recoil pion, the isobar subsequently decaying into a nucleon and pion.<sup>19</sup> Here we consider the ratios of different charge states that are involved under the assumption that a small number of compound states are involved in the photoproduction.

The isotopic spin wave functions are:

$$\begin{aligned} \psi(T=\frac{3}{2}) &= -(2/5)^{\frac{1}{2}}\psi_{+\frac{3}{2}\mu+1\eta-1} - (1/45)^{\frac{1}{2}}\psi_{-\frac{3}{2}\mu+1\eta_0} \\ &\quad - (2/45)^{\frac{1}{2}}\psi_{+\frac{3}{2}\mu_0\eta_0} + (16/45)^{\frac{1}{2}}\psi_{-\frac{3}{2}\mu_0\eta+1} \\ &\quad + (8/45)^{\frac{1}{2}}\psi_{+\frac{3}{2}\mu-1\eta+1}, \\ \psi(T=\frac{1}{2}) &= (\frac{1}{2})^{\frac{1}{2}}\psi_{+\frac{3}{2}\mu+1\eta-1} - (1/9)^{\frac{1}{2}}\psi_{-\frac{3}{2}\mu+1\eta_0} \\ &\quad - (2/9)^{\frac{1}{2}}\psi_{+\frac{3}{2}\mu_0\eta_0} + (1/9)^{\frac{1}{2}}\psi_{-\frac{3}{2}\mu_0\eta+1} \\ &\quad + (1/18)^{\frac{1}{2}}\psi_{+\frac{3}{2}\mu-1\eta+1}, \end{aligned}$$

where  $\psi_i$  represents the nucleon and  $\mu_i$  the pion from the decay of the isobar, and  $\eta_i$  is the recoil pion. The suffixes denote the  $z$  component of the isotopic spin. We are assuming that the isobar pion and the recoil pion in the isobar model are distinguishable particles. We ignore  $T=\frac{5}{2}$  as such a state cannot be made by electromagnetic interaction with a nucleon.<sup>20</sup> The total outgoing wave function is of the form

$$\phi_1\psi(T=\frac{1}{2}) + \phi_3\psi(T=\frac{3}{2}),$$

where the  $\phi$ 's are space-spin wave functions corresponding to the two isotopic spins. In the case that  $\phi_{1\rho e^{i\phi}} = \phi_3$ , the relative intensities of the different charge states are

$$\begin{aligned} (p+\pi^+) + \pi^- &= 1/2 + (2/5)\rho^2 - 2\frac{\rho}{5^{\frac{1}{2}}}\cos\phi = A, \\ (n+\pi^+) + \pi^0 &= 1/9 + (1/45)\rho^2 + (2/9)\frac{\rho}{5^{\frac{1}{2}}}\cos\phi = B, \\ (p+\pi^0) + \pi^0 &= 2/9 + (2/45)\rho^2 + (4/9)\frac{\rho}{5^{\frac{1}{2}}}\cos\phi = C, \\ (n+\pi^0) + \pi^+ &= 1/9 + (16/45)\rho^2 + (8/9)\frac{\rho}{5^{\frac{1}{2}}}\cos\phi = D, \\ (p+\pi^-) + \pi^+ &= 1/18 + (8/45)\rho^2 + (4/9)\frac{\rho}{5^{\frac{1}{2}}}\cos\phi = E. \end{aligned}$$

<sup>18</sup> M. Bloch, Ph.D. thesis, California Institute of Technology, 1958 (unpublished).

<sup>19</sup> R. M. Sternheimer and S. J. Lindenbaum, Phys. Rev. **109**, 1723 (1958).

<sup>20</sup> K. M. Watson, Phys. Rev. **85**, 852 (1952).

TABLE II. Differential cross sections for production of neutral pions in multiple-production reactions.

Photon energy (Mev)	Laboratory angle	Center-of-mass angle	Neutral pion kinetic energy range (c.m.)		$d^2\Omega/d\Omega dT$ (c.m.) (cm <sup>2</sup> sterad <sup>-1</sup> Mev <sup>-1</sup> )
			Minimum (Mev)	Maximum (Mev)	
990	60°	91°	175	295	$(3.44 \pm 1.20) \times 10^{-32}$
990	60°	91°	295	360	$(2.70 \pm 1.26) \times 10^{-32}$
990	86°	118°	80	215	$(2.76 \pm 1.32) \times 10^{-32}$
990	86°	118°	215	360	$(3.03 \pm 0.51) \times 10^{-32}$
810	86°	114°	75	195	$(1.47 \pm 0.78) \times 10^{-32}$
810	86°	114°	195	290	$(2.07 \pm 0.43) \times 10^{-32}$

Bloch and Sands<sup>18</sup> note that recoil negative pions are absent at 1000 Mev, which is surprising as this state has the largest coefficient in each isotopic spin wave function. In the case that  $\phi_{1\rho e^{i\phi}} = \phi_3$ , which could be so if both compound states involved are of the same spin and parity, one can destroy this charge state with  $\rho = (5/4)^{\frac{1}{2}}$ ,  $\phi = 0$ . For these values the ratio of yields of recoil neutral pions to isobar negative pions is  $(B+C)/E = 1.5$ . For photoproduction with 1000-Mev photons the recoil and isobar pions are quite well separated groups, so it seems justified to take the neutral pions we observe with kinetic energies between 180 and 360 Mev to be recoil pions. Combining this with the data of Bloch and Sands, we find an experimental value of  $1.05 \pm 0.4$  for this ratio. A best fit to all the three cross sections is obtained with

$$\begin{aligned} \rho &= 1.5, \quad \phi = 0^\circ, \quad \sigma(T=\frac{1}{2}) = 4.8 \mu\text{b-sterad}^{-1}, \\ \sigma(T=\frac{3}{2}) &= 10.9 \mu\text{b-sterad}^{-1}. \end{aligned}$$

The fact that isobar negative pions are weak at 660 Mev, together with the observation of a  $T=\frac{1}{2}$  resonance in single-pion photoproduction at about 750 Mev, suggests  $\rho=0$  at that energy while an intermediate value fits the meager data at 800 Mev. The results of this analysis are shown in detail in Table IV.

It has not been found possible to reduce the yield of recoil negative pions below that of isobar negative pions if the two compound states are of different spin or parity, though an exhaustive search has not been made. So this observation lends support to the idea that the two compound states have the same spin and parity, which is also suggested by the single positive pion cross sections (see Appendix).

This tentative analysis is based on very meager data but does seem to imply similar compound states to

TABLE III. Summary of cross sections for production of neutral pions in multiple-production reactions.

Photon energy (Mev)	Laboratory angle	Center-of-mass angle	Neutral pion kinetic energies (c.m.)		$d\sigma/d\Omega$ (c.m.) (cm <sup>2</sup> sterad <sup>-1</sup> )
			Minimum (Mev)	Maximum (Mev)	
990	60°	91°	175	360	$(5.9 \pm 1.6) \times 10^{-30}$
990	86°	118°	80	360	$(8.1 \pm 1.9) \times 10^{-30}$
810	86°	114°	75	290	$(3.7 \pm 1.0) \times 10^{-30}$

TABLE IV. Analysis of pion-pair photoproduction.  
Cross sections in  $\mu\text{b sterad}^{-1}$ .

Energy	660 Mev		800 Mev		1000 Mev	
$\rho$	0		0.5		1.5	
$\phi$	undetermined		45°		0°	
$\sigma(T=\frac{1}{2})$	8.0		10.5		4.8	
$\sigma(T=\frac{3}{2})$	0		2.7		10.9	
Cross sections	Calc	Obs	Calc	Obs	Calc	Obs
isobar $\pi^-$	0.4	<1.0	1.8	4.4±1.5	3.7	4.2±1.0
recoil $\pi^-$	4.0	3.9±1.0	3.0	...	0.3	<1.0
isobar $\pi^0$	2.7	...	6.8	...	10.1	...
recoil $\pi^0$	2.7	...	4.8	5.2±1.6	4.6	4.4±0.65
isobar $\pi^+$	4.9	...	4.6	7±3	1.8	3.6±3.4
recoil $\pi^+$	1.3	...	5.4	...	10.7	...

those involved in single pion photoproduction. Perhaps this discussion will at least provide ideas for some further experimental measurements.

#### ACKNOWLEDGMENTS

We are indebted to all the members of the Synchrotron Laboratory for contributions to this experiment, in particular to Dr. R. F. Bacher and Dr. R. L. Walker for their advice and encouragement. We are also indebted to Mr. A. Neubieser for his able operation of the synchrotron.

#### APPENDIX

An analysis has been made of the single-pion photoproduction data<sup>1-4,21,22</sup> assuming the following amplitudes to be involved:

- the classical resonance at 320 Mev, width 120 Mev,  $T=\frac{3}{2}$ ,  $J=\frac{3}{2}$ , amplitude= $Z=z$ ;
- a resonance at 750 Mev, width 120 Mev,  $T=\frac{1}{2}$ ,  $J=\frac{1}{2}+$ , amplitude= $Y_1=y_1e^{i\delta_1}$ ;
- a state at some higher energy,  $T=\frac{3}{2}$ ,  $J=\frac{1}{2}+$ , amplitude= $Y_2=y_2e^{i\delta_2}$ ;
- the  $s$ -wave production of  $\pi^+$ 's which is already well known up to 500 Mev, amplitude= $X=xe^{i\alpha}$ .

The use of the word "resonance" simply implies that the amplitudes  $Z$ ,  $Y_1$  vary with energy like

$$[(E-E_r)-\frac{1}{2}i\gamma]^{-1}.$$

The arguments on which these assignments are based are, in order as follows:

(1) The assignments of isotopic spins are obvious from the ratios of cross sections for positive- and neutral-pion production.

(2) The angular distributions in neutral-pion production are, to a good approximation, symmetric about 90° implying that the main orbital angular

<sup>21</sup> F. P. Dixon and R. L. Walker, Phys. Rev. Letters 1, 142 (1958).

<sup>22</sup> Heineberg, McClelland, Turkot, Woodward, Wilson, and Zipoy, Phys. Rev. 110, 1211 (1958).

momenta involved are of the same parity. As the classical resonance at 320 Mev must still be making an important contribution right up to 1000 Mev, this implies that the outgoing mesons from the other states must be  $p$ ,  $f$ , ... wave. The simplest assumption is  $p$ -wave, with possible compound states  $\frac{1}{2}+$ ,  $\frac{3}{2}+$ .

(3) The angular distributions in positive-ion production have a strong  $\cos\theta$  term in the region 600-800 Mev. In addition to the angular momenta introduced in (2) there must also be some  $s$ ,  $d$ , ... wave. The simplest assumption is to continue the  $s$ -wave positive-pion production which is already well known below 500 Mev.

(4) The resonance at 750 Mev is quite pronounced in the positive-pion cross section at 90° and one sees that the fall-off on the high-energy side is steep. One would like to ascribe this to an interference between states (b) and (c) of the same spin and parity. Similarly one would like to ascribe the absence of recoil negative pions at 1000 Mev to a similar interference. If  $\frac{3}{2}+$  is chosen, all three states (a), (b), and (c) have the same spin and parity and the neutral-pion angular distribution would be throughout of the form  $(5-3\cos^2\theta)$  which is contradicted by the observation of a positive coefficient of the  $\cos^2\theta$  term at 940 Mev. This leaves us with an assignment of  $\frac{1}{2}+$  for the states (b) and (c).

To prove that these assignments are possible, a detailed fit has been made to the angular distributions, using

$$W(\theta) = |X|^2 + |Y|^2 + \frac{1}{2}|Z|^2(5-3\cos^2\theta) - 2\text{Re}[X^*(Z-Y)]\cos\theta - \text{Re}(Y^*Z)(3\cos^2\theta-1),$$

with  $Y=Y_1+Y_2$ . The amplitudes used in fitting are given in Table V and the resultant angular distributions are given in Table VI. It will be noted in Table V that the ratios of corresponding amplitudes for production of positive and neutral pions at the same energy have been chosen in agreement with the isotopic spin assignments to the states concerned.

It is further noted that the reaction  $\gamma+p \rightarrow K^+\Lambda^0$  can only proceed through a  $T=\frac{1}{2}$  compound state. It

TABLE V. Amplitudes used in fitting single-pion photoproduction.

Energy (Mev)	(a) for $\gamma+p \rightarrow p+\pi^0$						
	$x$	$z$	$y_1$	$\delta_1$	$y_2$	$\delta_2$	
600	0	1.02	0.55	-30°	0	...	
700	0	0.80	1.21	0°	0	...	
800	0	0.62	1.14	85°	0.50	75°	
940	0	0.48	0.42	130°	0.90	130°	
Energy (Mev)	(b) for $\gamma+p \rightarrow n+\pi^+$						
	$x$	$\alpha$	$z$	$y_1$	$\delta_1$	$y_2$	$\delta_2$
600	2.30	-165°, 133°	0.72	0.78	150°	0	...
700	2.19	-130°, 128°	0.565	1.71	180°	0	...
800	1.52	-85°, 225°	0.44	1.61	265°	0.35	75°
900	1.45	-25°, 85°	0.35	0.75	290°	0.56	105°
1000	1.26	70°, 280°	0.30	0.48	295°	0.76	140°



is tempting to ascribe the observed cross sections<sup>6,23,24</sup> to the tail of the resonance at 750 Mev. This might then explain the rapid rise of the cross section above threshold, and the isotropy would support our assignment of  $J=\frac{1}{2}$ . The data can probably also be fitted with the model of Gell-Mann<sup>25</sup> where  $K^+$  photoproduction is just  $\pi^+$  photoproduction over again with a smaller coupling constant.

In this model the cross sections would be fitted with an  $s$ -wave amplitude similar to that in the photoproduction of positive pions near threshold. The difference between the two models lies in the predictions for the cross section for the reaction  $\gamma+n \rightarrow K^0+\Lambda^0$ . If due to the 750-Mev resonance it would be approximately as strong as the  $K^+$  cross section while in Gell-Mann's model it would be much weaker. An experimental decision in favor of either of these models may perhaps

<sup>23</sup> Brody, Wetherell, and Walker, Phys. Rev. **110**, 1213 (1958).

<sup>24</sup> McDaniel, Silverman, Wilson, and Cortellessa, Phys. Rev. Letters **1**, 109 (1958).

<sup>25</sup> M. Gell-Mann, Phys. Rev. **106**, 1296 (1957).

TABLE VI. Angular distributions calculated in analysis of single-pion photoproduction, expressed in  $\mu\text{b sterad}^{-1}$ .

(a) for $\gamma+p \rightarrow p+\pi^0$	
600 Mev:	$3.4-3.0 \cos^2\theta$
700 Mev:	$4.0-3.9 \cos^2\theta$
800 Mev:	$3.5-1.0 \cos^2\theta$
940 Mev:	$1.9+0.9 \cos^2\theta$
(b) for $\gamma+p \rightarrow n+\pi^+$	
600 Mev:	$6.7+5.7 \cos\theta+0.7 \cos^2\theta$
700 Mev:	$7.55+6.4 \cos\theta+2.4 \cos^2\theta$
800 Mev:	$4.4+3.7 \cos\theta-0.2 \cos^2\theta$
900 Mev:	$2.5-0.7 \cos\theta-0.3 \cos^2\theta$
1000 Mev:	$1.8-0.5 \cos\theta+0.2 \cos^2\theta$

cast some light on the  $K$ -meson parity. Gell-Mann's model requires a pseudoscalar  $K$  meson, while in our model the steep rise in the cross section above threshold would probably imply  $s$ -wave production which, if due to the  $\frac{1}{2}^+$  resonance, would imply a scalar  $K$  meson.

I am indebted to Dr. R. L. Walker for illuminating conversations about this analysis.

## Helicity of the Electron and Positron in Muon Decay\*

PIERRE C. MACQ,† KENNETH M. CROWE, AND ROY P. HADDOCK  
Radiation Laboratory, University of California, Berkeley, California

(Received August 29, 1958)

The helicity of the electron and positron from muon decay has been measured by determining the sense of circular polarization of their bremsstrahlung by the method of absorption in iron magnetized against or along the direction of motion of the particles. The positron is found to be right-handed and the electron left-handed.

The results are consistent with the two-component neutrino theory, which assumes ( $V,A$ ) interaction, conservation of leptons, and left-handed neutrinos.

### I. INTRODUCTION

SINCE Lee and Yang advanced the hypothesis of the violation of the parity-conservation law in physical phenomena proceeding from weakly interacting particle fields,<sup>1</sup> vigorous theoretical and experimental efforts have been made to clarify understanding of weak interactions. This hypothesis of parity non-conservation doubled the already large number of independent parameters required to describe weak interactions. Landau, Lee, Yang, and Salam have reinvestigated the old and appealing two-component neutrino theory and have shown on the basis of this theory that the number of parameters is halved once we are able to determine the helicity of the neutrino.<sup>2</sup>

\* Work done under the auspices of the U. S. Atomic Energy Commission.

† On leave of absence from the University of Louvain, Belgium.

<sup>1</sup> T. D. Lee and C. N. Yang, Phys. Rev. **104**, 254 (1956).

<sup>2</sup> L. Landau, Nuclear Phys. **3**, 127 (1957); T. D. Lee and C. N. Yang, Phys. Rev. **105**, 1671 (1957); A. Salam, Nuovo cimento **5**, 299 (1957).

In the following discussion we assume that the two-component theory applies.

The experiments on the electron distribution from oriented beta sources, on polarization measurements, and on the absence of interference effects in the spectrum shape<sup>3</sup> lead to two possibilities for  $\beta$  decay:

(a) it is of the  $V$  and  $A$  form of interaction, and emits left-handed neutrinos (the neutrino is defined as the neutral particle emitted in the bound-proton decay), or

(b) it is of the  $S$ ,  $T$ , and  $P$  form of interaction, and emits right-handed neutrinos.

A clear choice between these two classes for  $\beta$  decay has been made by Goldhaber *et al.*<sup>4</sup> They have measured the polarization of the neutrino in electron  $K$  capture by the method of resonance scattering of the  $\gamma$  ray.

<sup>3</sup> See, for example, the general bibliography given by M. Gell-Mann and A. Rosenfeld, *Annual Review of Nuclear Science* (Annual Reviews, Inc., Stanford, 1957), Vol. 7, p. 407.

<sup>4</sup> Goldhaber, Grodzins, and Sunyar, Phys. Rev. **109**, 1015 (1958).